Valeology: International Journal of Medical Anthropology and Bioethics
(ISSN 2995-4924) VOLUME 03 ISSUE 6, 2025

THEORETICAL STUDY OF MOLECULAR AND SPECTRAL PROPERTIES OF SOME COMPOUNDS

Qudama Kh. Hammad, Adil N. Ayyash
University of Anbar, College of Science, Department of Physics, Anbar, Iraq

Abstract:

In this study, the spectral and molecular parameters are calculated by some molecular programs to obtain of the results of our compounds. The various properties of the ground and excited electronic states of The pyrromethene 580 molecule was theoretically simulated in this study utilizing density functional theory (DFT) and the B3LYP at a 6-31 G (d,p) basis set. Then, bond lengths and bond angles were determined using DFT methods, The electronic properties such as the electronic energy, dipole moments, such as ionization potentials (IP), absolute softness (S), chemical potential (K), electrophilic index (ω), electron affinities (EA), absolute hardness (η), Molecular electrostatic potential (MEP) and Absorption spectra. The energy values were -1192.534269 Hartree. The dipole moment values found to be 3.96 Debye indicate the non-uniform distribution of charges. The energy gap was found to be 2.96 eV, which reflected the stability of the molecule. We find good agreement between experimental and theoretical data of UV spectrum where λ_max theoretically with solvent ethanol was 513 nm and experimentally was 519-522 dependent on the change in concentration

Introduction

1. Introduction

A class of extremely effective laser dyes called as pyrromethenes (PMs) (Boron- dipyrromethene dyes), sometimes referred to as BODIPY, are fluorescent dyes utilized in laser applications [1, 2]. They are made of dipyrromethene complexed with a boron atom that has undergone two substitutions, usually a BF2 atom. A group of dyes with a bonded boron atom in their center are all built from a core structure with a boron-dipyrromethene tricyclic ring system. An important group of laser dyes are BODIPYs. They have tunable electromagnetic properties in the visible green-yellow spectrum. They have a large molar absorption co-efficiency, high lasing efficiency, good photostability, high fluorescence quantum yield, and a low rate constant of intersystem crossover.

Although they are known for having sharp excitation and emission peaks, they also have a relatively tiny Stokes shift and can be sensitive to environmental factors, such as dye-dye quenching effects, which can modify the brightness of the material. [3, 4]. By include the appropriate replacement in the molecular structure of the parent BODIPY chromophore, it is possible to modify the photophysical properties of these dyes to some extent. There are some BODIPY complexes that may be purchased commercially. The. Pyromethene-567 (PM 567) is the brand name given to the compound of 1,3,5,7,8- pentamethyl-2,6-diethyl- BODIPY that lases at 547 nm. Pyromethene-580 is the brand name for the 1,3,5,7,8-pentamethyl-2,6-di-n-butylpyrromethene-difluoroborate complex (PM 580). Figure (1) illustrates the structure of PM 580 (C22H33BF2N2) [5]

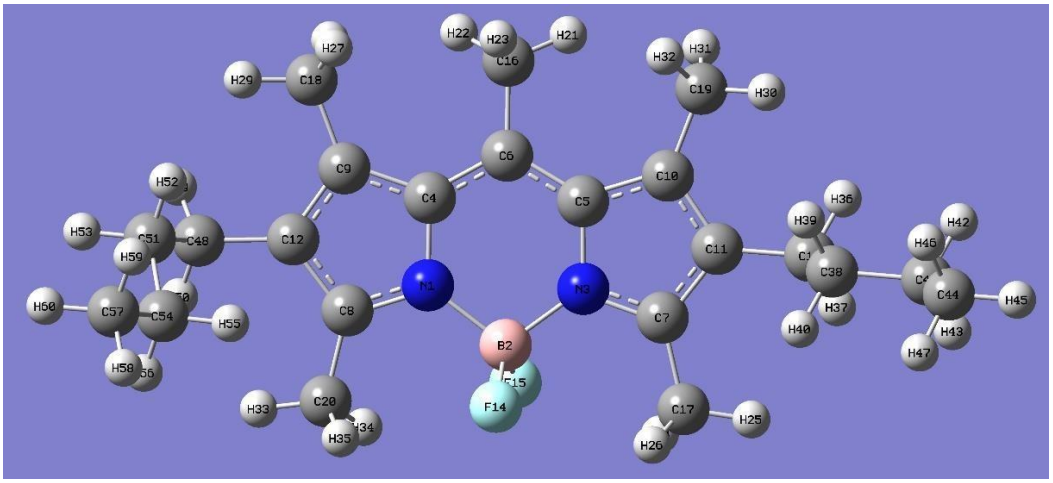

(Fig.1) Optimized geometric structure of the bond length PM580 by B3LYP

Numerous investigations have demonstrated the accuracy of the density functional theory DFT methods' calculations of molecule structures and vibration frequencies . Density functional theory is now one of the methods for estimating the ground state electronic structure in quantum chemistry and solid state physics (DFT). Modern density functional approaches exhibit a good balance between accuracy and computing efficiency compared to classical ab initio [6, 7].

The structure, electronic properties, and electronic spectra of PM-580 in ethanol solvents are investigated in the current work using an experimental and theoretical methodology called the TDDFT method

2. Computational methods: -

Pyrromethene 580 dye laser (PM-580) supplied from British Drug Houses (BDH), Sigma-Aldrich has a molecular mass (374.32 gm/mole), molecular formula (C22H33BF2N2) .

In the current work, we pay close attention to how DFT and TDDFT are applied to the PM-580. At the B3LYP/6-31G(d,p) levels of theory, the (DFT & TDDFT) approach was used to conduct all computational studies. This research of PM-580 was performed on a home computer using the Gaussian 09 algorithm and the Gauss-View molecular visualization software suite [8, 9].

The B3LYP functional with gradient correction. Any molecules' electronic excitations and UV-Vis spectra were calculated using time-dependent density functional theory (TD- DFT) methods at the B3LYP/6-31G(d,p) level. The most accurate way to determine ground state structures and electrical variables is using DFT.. The results of the (TD- DFT) calculations of energy and oscillator strength support the experimental results. Without any symmetry restrictions, restricted closed-shell formalism is used to create the geometry-optimized structures. The more pertinent ionization potential (IP), electron affinities (EA), chemical potential (K)—which is the opposite of electronegativity (χ), softness (S), electrophilic index (ω) and the dipole moment (μ) hardness (η), were all determined for this inquiry. These are demonstrating the molecular electrostatic potential as

well as the charge transport within the molecule (MESP) The contour map of the molecule in the title displays its many electrophilic regions. [10]. In the context of Koopmans' theorem, the IP and EA were estimated using the HOMO and LUMO energy.

$$: IP=-\varepsilon HOMO \text{ and } EA=-\varepsilon LUMO \ldots\ldots (1)[11].$$

All parameters are calculated as follows [12-16]:

$$\text{Electronegativity } (\chi),\ \chi = \frac{IP+EA}{2} \ldots\ldots (2)$$

$$\text{Hardness } (\eta) = \frac{IP-EA}{2} \ldots\ldots (3)$$

$$\text{Softness } S = \frac{1}{y} \ldots\ldots (4)$$

$$\text{Electrophilic index } \omega = \frac{-\chi^2}{2y} \ldots\ldots (5)$$

The dipole moment in a molecule, which is an important aspect since the stronger the intermolecular contacts are, the higher the dipole moment, is frequently used in the study of intermolecular interactions involving nonbonded type dipole-dipole interactions [17, 18]

3. Results and Discussion

a. Bond Lengths

The usual distance between the nuclei of two bound atoms in a molecule is known as the bond distance, bond length, or internuclear distance in molecular geometry. It is a characteristic of the atomic bond that can be transferred. Bond order determines bond length, which decreases as the number of electrons involved in bond formation rises. The bond strength and bond dissociation energy are inversely correlated with the bond length or distance. A tougher bond is smaller when all the elements that affect bond strength are considered. Picometers (1 pm = 10^{-12} m) or Angstroms (1 = 10^{-10} m) are used to measure bond distances. [19].

Table (1) Selected bond length (Å) of PM580 at B3LYP methods

Code	*Assignment*	*Value*
R1	N1-B2	1.554
R2	N1-C4	1.3962
R3	N1-C8	1.3469
R4	B2-N3	1.5547
R5	B2-F14	1.3947
R6	B2-F15	1.3956
R7	N3-C5	1.3968
R8	N3-C7	1.3455
R9	C4-C6	1.4095
R10	C4=C9	1.4338
R11	C5=C6	1.4083
R12	C5-C10	1.4354
R13	C6-C16	1.5085
R14	C7=C11	1.4176
R15	C7-C17	1.4946
R16	C8=C12	1.4176
R17	C8-C20	1.495
R18	C9-C12	1.4003
R19	C9-C18	1.5026

R20	C10-C11	1.3986
R21	C10-C19	1.5025
R22	C11-C13	1.505
R23	C12-C48	1.5071
R24	C13-H36	1.0968
R25	C13-H37	1.0973
R26	C13-C38	1.5424
R27	C16-H21	1.0871
R28	C16-H22	1.0875
R29	C16-H23	1.0976
R30	C17-H24	1.0938
R31	C17-H25	1.0912
R32	C17-H26	1.0944
R33	C18-H27	1.0946
R34	C18-H28	1.0971
R35	C18-H29	1.0917
R36	C19-H30	1.0921
R37	C19-H31	1.0972
R38	C19-H32	1.0943
R39	C20-H34	1.0907
R40	C20-H35	1.0937
R41	C20-H36	1.0943
R42	C38-H39	1.0984
R43	C38-H40	1.0982
R44	C38-C41	1.5331
R45	C41-H42	1.0988
R46	C41-H43	1.0986
R47	C41-C44	1.5315
R48	C44-H45	1.0948
R49	C44-H46	1.0959
R50	C44-H47	1.0958
R51	C48-H49	1.0967
R52	C48-H50	1.0965
R53	C48-C51	1.5463
R54	C51-H52	1.0984
R55	C51-H53	1.0987
R56	C51-C54	1.5327
R57	C54-H55	1.0968
R58	C54-H56	1.0986
R59	C54-C57	1.5317
R60	C57-H58	1.0948
R61	C57-H59	1.096
R62	C57-H60	1.0961

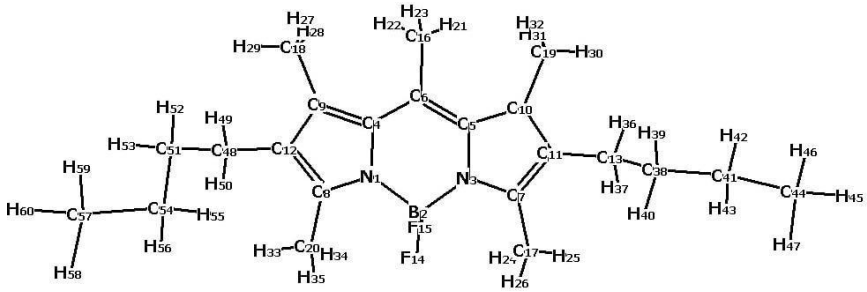

Fig (2). Optimized geometric structure of the bond length PM580 by B3LYP

b. Bond Angles

Any angle between two bonds that share an atom is known as a bond angle, and it is often measured in degrees. Table (2) lists the elected bond angles determined by DFT techniques.

Table (2) Selected bond angles (degree) for PM580

Code	Assignment	Value	Code	Assignment	Value
A1	B2-F14	126.0748	**A60**	C9-C18-H29	110.3819
A2	B2-N1-C8	124.8466	**A61**	H27-C18-H28	107.181
A3	C4-N1-C8	109.07	**A62**	H27-C18-H29	107.238
A4	N1-B2-N3	106.1214	**A63**	H28-C18-H29	106.8725
A5	N1-B2-F14	109.9479	**A64**	C10-C19-H30	110.3379
A6	N1-B2-F15	110.3256	**A65**	C10-C19-H31	112.5035
A7	A(3,2,14)	109.8496	**A66**	C10-C19-H32	112.36
A8	) N3-B2-F15	110.205	**A67**	H30-C19-H31	106.8915
A9	F14-B2-F15	110.3095	**A68**	H30-C19-H32	107.1925
A10	B2-N3-C5	126.1243	**A69**	H31-C19-H32	107.2515
A11	B2-N3-C7	124.8222	**A70**	C8-C20-H33	111.2692
A12	C5-N3-C7	109.0426	**A71**	C8-C20-H34	110.0408
A13	N1-C4-C6	120.3731	**A72**	C8-C20-H35	110.5267
A14	N1-C4=C9	107.3435	**A73**	H33-C8-H34	109.3034
A15	C6-C4=C9	132.276	**A74**	H33-C20-H35	108.9313
A16	N3-C5=C6	120.304	**A75**	H34-C20-H35	106.6486
A17	N3-C5-C10	107.3316	**A76**	C13-C38-H39	109.1528
A18	C6=C5-C10	132.3595	**A77**	C13-C38-H40	109.1351
A19	C4-C6=C5	120.7015	**A78**	C13-C38-C41	113.2032
A20	C4-C6-C16	119.577	**A79**	H39-C38-C41	105.8258
A21	C5=C6-C16	119.721	**A80**	H39-C38-C41	109.6365
A22	N3-C7=C11	109.5967	**A81**	H40-C38-C41	109.6205
A23	N3-C7-C17	121.7253	**A82**	C38-C41-H42	109.2462
A24	C11=C7-C17	128.678	**A83**	C38-C41-H43	109.2206
A25	N1-C8=C12	109.5665	**A84**	C38-C41-C44	113.2292
A26	N1-C8-C20	121.3729	**A85**	H42-C41-H43	105.9208
A27	C12=C8-C20	129.0582	**A86**	H42-C41-C44	109.4692
A28	C4=C9-C12	106.9777	**A87**	H43-C41-C44	109.4938
A29	C4=C9-C18	128.8587	**A88**	C41-C44-H45	111.4506
A30	C12-C9-C18	124.1595	**A89**	C41-C44-H46	111.199
A31	C5-C10-C11	106.9043	**A90**	C41-C44-H47	111.2194
A32	C5-C10-C19	128.8604	**A91**	H45-C44-H46	107.6593

A33	C11-C10-C19	124.2177	**A92**	H45-C44-H47	107.6577
A34	C7=C11-C10	107.1205	**A93**	H46-C44-H47	107.4618
A35	C7=C11-C13	125.2251	**A94**	C12-C48-H49	109.3303
A36	C10-C11-C13	127.637	**A95**	C12-C48-H50	109.455
A37	C8=C12-C9	107.0368	**A96**	C12-C48-C51	115.1181
A38	C=C12-C48	126.0815	**A97**	H49-C48-H50	105.3593
A39	C9-C12-C48	126.8809	**A98**	H49-C48-C51	108.4692
A40	C11-C13-H36	109.8647	**A99**	H50-C48-C51	108.6564
A41	C11-C13-H37	109.4652	**A100**	C48-C51-H52	109.222
A42	C11-C13-C38	114.0632	**A101**	C48-C51-H53	108.3656
A43	H36-C13-H37	105.3305	**A102**	C48-C51-C54	114.5579
A44	H36-C13-C38	108.9832	**A103**	H52-C51-H53	106.183
A45	H37-C13-C38	108.7628	**A104**	H52-C51-C54	109.0637
A46	C6-C16-H21	111.4742	**A105**	H53-C51-C54	109.1172
A47	C6-C16-H22	111.3144	**A106**	C51-C54-H55	109.4066
A48	C6-C16-H23	111.3131	**A107**	C51-C54-H56	109.2164
A49	H21-C16-H22	107.4448	**A108**	C51-C54-H57	112.9138
A50	H21-C16-H23	107.586	**A109**	H55-C54-H56	106.2104
A51	H22-C16-H23	107.5005	**A110**	H55-C54-C57	109.5021
A52	C7-C17-H24	110.1741	**A111**	H56-C54-C57	109.3698
A53	C7-C17-H25	111.1626	**A112**	C54-C57-H58	111.4152
A54	C7-C17-H26	110.4648	**A113**	C54-C57-H59	111.1931
A55	H24-C17-H25	109.2726	**A114**	C54-C57-H60	111.2948
A56	H24-C17-H26	106.6008	**A115**	H58-C57-H59	107.6032
A57	H25-C17-H26	109.0482	**A116**	H58-C57-H60	107.6585
A58	C9-C18-H27	112.4859	**A117**	H59-C57-H60	107.4811
A59	C9-C18-H28	112.3757			

c. Electronic properties

The lowest unoccupied molecular orbital (LUMO) serves predominantly as the electron acceptor, while the highest occupied molecular orbital (HOMO) serves primarily as the electron donor [20, 21]. The eigenvalues of LUMO and HOMO and their energy gap are indicators of the molecule's chemical activity. The ability to get an electron is represented by LUMO as an electron acceptor, while the ability to donate an electron is represented by HOMO as an electron donor [22, 23]. Higher HOMO energies make it easier to donate electrons, and lower LUMO energies make it easier to take electrons, so the smaller the LUMO-HOMO energy gaps, the easier it is to excite HOMO electrons. [24, 25]. The values of the total energy, electronic states, energy gap (LUMO-HOMO), and dipole moment (μ) of the PM-580 for the pyrromethene-580 molecule are shown in Table (3). 3.961364 Debye is the measured ground-state dipole moment in the experiment. The electronic properties of the organic molecules under study, such as absolute softness (S), ionization potentials (IP), absolute hardness (η), electron affinities (EA), chemical potential (K), electrophilic index (ω) can be calculated with high accuracy using the B3LYP functional used in this study..

Table (3) Electronic properties of PM-580

Property	**TD-DFT B3LYP/6-31G (d,p)**
IP (eV)	5.18008
EA (eV)	2.21968
χ (eV)	3.69988

ω(**eV**)	4.62407513
ε(eV^{-1})	0.216259462
η (eV)	1.4802
S (eV^{-1})	0.67558438
$\mathbf{C_p}$ (eV)	-3.69988
Etot (a.u.)	-1192.534269
EHOMO (eV)	-5.18008
ELUMO (eV)	-2.21968
EGap(eV)	2.960393 eV

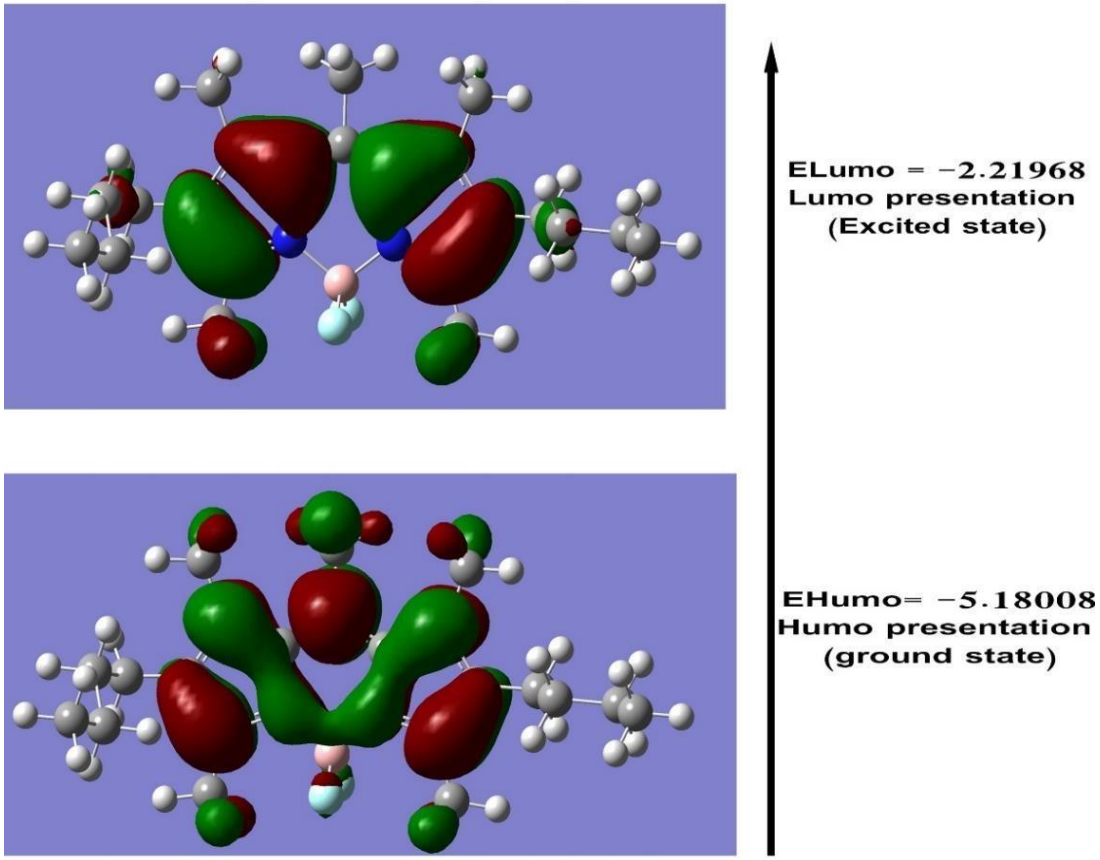

Fig. (3). Optimized geometric structure of the bond length PM580

d. Molecular electrostatic potential (MEP)

According to dipole moments, electronegativity, partial charges, and chemical reactivity of the molecules, the molecular electrostatic potential (ESP) at a point in the space around a molecule indicates the net electrostatic effect produced at that location by the total charge distribution (electron + nuclei) of the molecule [26, 27] .

The interactions between molecules can be predicted using the charge distributions. Finding the reactive site of a molecule is one of the goals of determining the electrostatic potential. Figure displays the three-dimensional electrostatic potential maps of the PM-580 (4). Electrophilic assault can occur on a region of the molecule that has a negative electrostatic potential. The negative and positive electrostatic potential regions are represented by the EPS map's red and blue regions, which correspond to the regions that are respectively electron-rich and electron-deficient. The neutral electrostatic potential zone is represented by the green color. [28, 29].

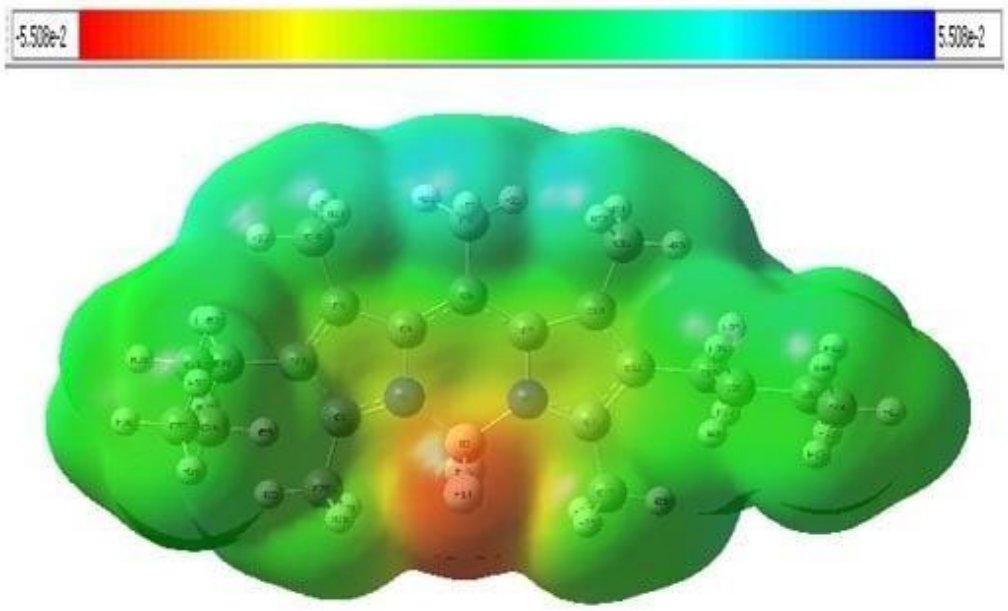

Fig. (4). Molecular electrostatic potential mappedonto a surface of total electron density for PM-580

e. Absorption spectra

Figures (5) depict the shift in wavelength observed between 300 and 800 nm using UV technology. The molecular orbital structure where the primary electron transition is seen in the electronic absorption spectra of the PM 580 at λmax = 513 nm. On the oscillator strength for this approach, a significant absorption peak is seen (f = 0.36). These findings are in agreement with the experimental measurement, which was between 519 and 522 nm.

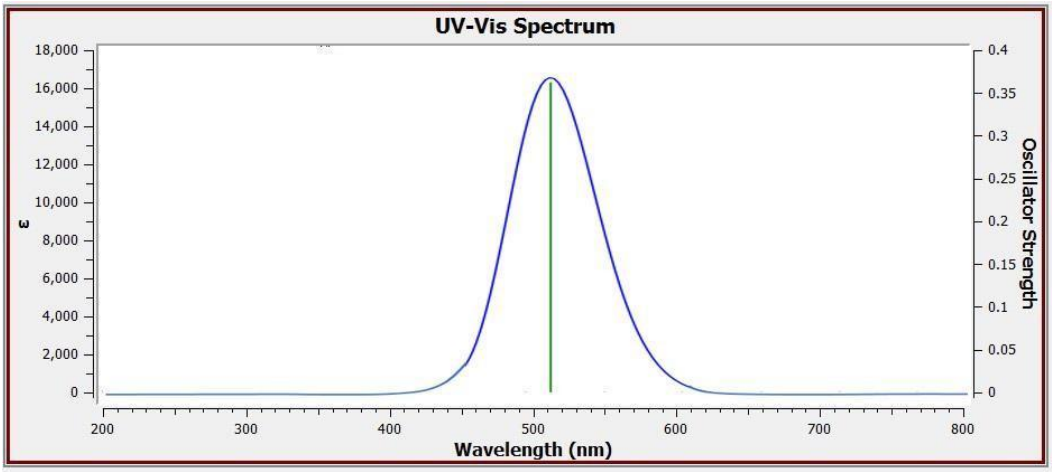

Fig (5). TD-B3LYP -UV spectrum of the PM 580

4. Conclusions

By utilizing the DFT/TDDFT methodologies and accounting for the solvent effect in the absorption spectra, the structures and electronic spectra of pyrromethene 580 have been examined in this work. Our findings suggest that TDDFT is an effective method for addressing the spectroscopy and characteristics of the pyrromethene 580 Excitation state. The compound's excitation energy, oscillator strength, and maximum absorption wavelength (max) were all calculated using TD-DFT techniques. The oscillator strength and absorption wavelength were then compared to experimental method values to see if there was agreement.

References

1. T. G. Pavlopoulos, J. H. Boyer, K. Thangaraj, G. Sathyamoorthi, M. P. Shah, and M.-L. Soong, "Laser dye spectroscopy of some pyrromethene-BF 2 complexes," *Applied optics,* vol. 31, no. 33, pp. 7089-7094, 1992.
2. A. E. Wertz, "Bimetallic Ruthenium (II) Polypyridyl Complexes Bridged by a Boron Dipyrromethene (BODIPY): Synthesis, Spectroscopic and Plasmid DNA Photoreactions and The Impact of the 515 nm Effect in Photosynthesis: Model System Using β-Carotene Acid Complexes," University of Dayton, 2019.
3. L. R. Morgan, A. Chaudhuri, L. E. Gillen, J. H. Boyer, and L. T. Wolford, "Pentamethylpyrromethene boron difluoride complexes in human ovarian cancer photodynamic therapy," in *Photodynamic Therapy: Mechanisms II*, 1990, vol. 1203: SPIE, pp. 253-265.
4. G. T. J. B. t. Hermanson, "Fluorescent probes," vol. 3, pp. 395-463, 2013.
5. G. Shankarling and K. J. R. Jarag, "Laser dyes," vol. 15, no. 9, pp. 804-818, 2010.
6. F. Furche and D. Rappoport, "III. Density functional methods for excited states: Equilibrium structure and electronic spectra," *Computational photochemistry,* vol. 16, pp. 93-128, 2005.
7. H. Li *et al.*, "Deep-learning density functional theory Hamiltonian for efficient ab initio electronic-structure calculation," *Nature Computational Science,* vol. 2, no. 6, pp. 367-377, 2022.
8. M. Frisch *et al.*, "Gaussian 09, rev," *Gaussian Inc, Wallingford,* 2009.
9. Y. Samuel, A. Garg, and E. Mulugeta, "Synthesis, DFT Analysis, and Evaluation of Antibacterial and Antioxidant Activities of Sulfathiazole Derivatives Combined with In Silico Molecular Docking and ADMET Predictions," *Biochemistry Research International,* vol. 2021, 2021.
10. L. S. Ahamed, R. A. Ali, R. S. Ahmed, M. R. Ahamad, and R. I. Al-Bayati, "Synthesis of New7-ethyl-4-methyl-2-Quinolone Derivatives," *Al-Nahrain Journal of Science,* no. 2, pp. 30-37, 2019.
11. M. M. Kadhim and R. M. Kubba, "Theoretical investigation on reaction pathway, biological activity, toxicity and NLO properties of diclofenac drug and its ionic carriers," *Iraqi Journal of Science,* pp. 936-951, 2020.
12. F. Mutlak, A. T. Mohi, and T. J. Alwan, "Density functional theory study of molecular structure, Electronic properties, UV–Vis spectra on coumarin102," *Baghdad Science Journal,* vol. 13, no. 143-152, 2016.
13. E. Wahab, E. M. Ahmed, Y. Rammah, and K. S. Shaaban, "Basicity, electronegativity, optical parameters and radiation attenuation characteristics of P2O5-As2O3-PbO glasses doped vanadium ions," *Journal of Inorganic and Organometallic Polymers and Materials,* pp. 1-14, 2022.
14. A. Deshpande *et al.*, "Quantum Computational Supremacy via High-Dimensional Gaussian Boson Sampling," *arXiv preprint arXiv:2102.12474,* 2021.
15. A. Bekshaev and L. Mikhaylovskaya, "Displacements of optical vortices in Laguerre–Gaussian beams diffracted by a soft-edge screen," *Optics Communications,* vol. 447, pp. 80-88, 2019.
16. R. Pal and P. K. Chattaraj, "Electrophilicity index revisited," *Journal of Computational Chemistry,* 2022.

17. S. R. Kumar, N. Vijay, K. Amarendra, P. Onkar, and S. Leena, "Theoretical Studies on the Isomers of Quinazolinone by first Principles," *Research Journal of Recent Sciences _ ISSN*, vol. 2277, p. 2502, 2012.

18. M. Miar, A. Shiroudi, K. Pourshamsian, A. R. Oliaey, and F. Hatamjafari, "Theoretical investigations on the HOMO–LUMO gap and global reactivity descriptor studies, natural bond orbital, and nucleus-independent chemical shifts analyses of 3-phenylbenzo [d] thiazole-2 (3 H)-imine and its para-substituted derivatives: Solvent and substituent effects," *Journal of Chemical Research*, vol. 45, no. 1-2, pp. 147-158, 2021.

19. N. K. Rasheed and A. N. Ayaash, "A Comparative Study of Potential Energy Curves Analytical Representations for CO, N2, P2, and ScF in Their Ground Electronic States," *Iraqi Journal of Science*, pp. 2536-2542, 2021.

20. P. Priya, C. Kala, and D. Thiruvadigal, "Investigation on the influence of substitute groups in organic nanodevices," *Int. J. Nanoelectronics and Materials*, vol. 3, pp. 1-7, 2010.

21. C. Sun *et al.*, "High efficiency polymer solar cells with efficient hole transfer at zero highest occupied molecular orbital offset between methylated polymer donor and brominated acceptor," *Journal of the American Chemical Society*, vol. 142, no. 3, pp. 1465-1474, 2020.

22. A. Dhumad, "Theoretical study for Synthesis Reactions of α-Alkylidene-γ- butyrolacton-2-ones (Tetronic acid Derivatives)," *Journal of Basrah Researches (Sciences)*, vol. 37, no. 5, pp. 82-89, 2011.

23. J. Miao, H. Li, T. Wang, Y. Han, J. Liu, and L. Wang, "Donor–acceptor type conjugated copolymers based on alternating BNBP and oligothiophene units: from electron acceptor to electron donor and from amorphous to semicrystalline," *Journal of Materials Chemistry A*, vol. 8, no. 40, pp. 20998-21006, 2020.

24. Z. Wang and S. Wu, "Electronic structures and spectra of conducting anthracene derivatives," *Journal of the Serbian Chemical Society*, vol. 73, no. 12, pp. 1187- 1196, 2008.

25. A. A. Ibrahim, M. A. Ibrahim, E. A. Sulliman, S. M. Daood, and G. Q. Ismael, "Comparison study of HOMO-LUMO energy gaps for tautomerism of triazoles in different solvents using theoretical calculations," *NTU Journal of Pure Sciences*, vol. 1, no. 1, pp. 38-43, 2021.

26. B. D. Joshi, P. Tandon, and S. Jain, "Molecular characterization of yohimbine hydrochloride using vibrational spectroscopy and quantum chemical calculations," *BIBECHANA*, vol. 8, pp. 73-80, 2012.

27. S. Lakshminarayanan, V. Jeyasingh, K. Murugesan, N. Selvapalam, and G. Dass, "Molecular electrostatic potential (MEP) surface analysis of chemo sensors: An extra supporting hand for strength, selectivity & non-traditional interactions," *Journal of Photochemistry and Photobiology*, vol. 6, p. 100022, 2021.

28. M. Murugana, V. Balachandrana, and M. Karnan, "Vibrational spectra and electrostatic potential surface of 2-fluoro-6-methoxybenzonitrile based on quantum chemical calculations," *J. Chem. Pharm. Res*, vol. 4, no. 7, pp. 3400- 3413, 2012.